

1 **Identification of Low-Level Jets from AWAKEN Lidar Data**

2

3 C. Alexander Hirst^a

4 ^a *University of Colorado Boulder, Boulder, Colorado, U.S.A*

5

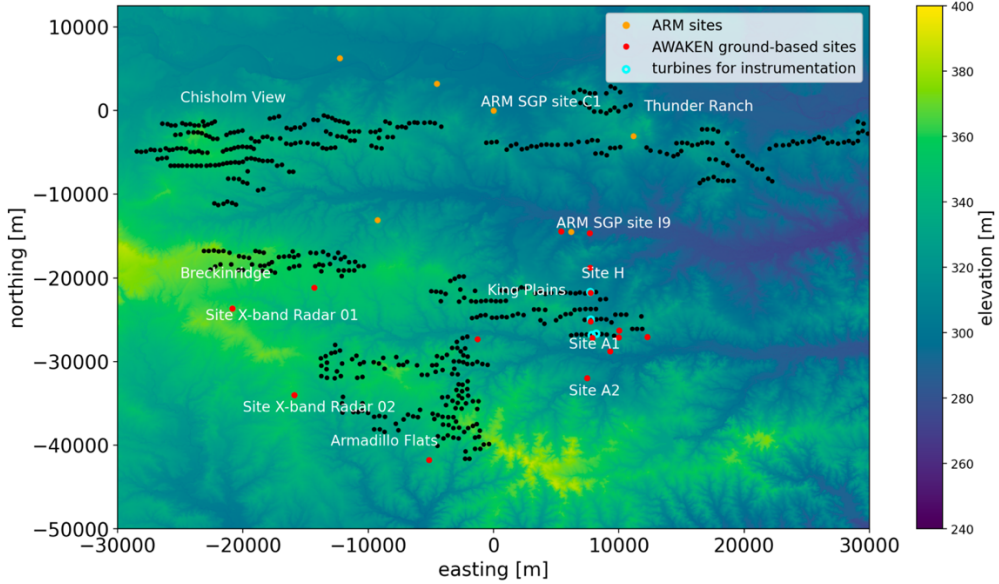
6 *Corresponding author:* C. Alexander Hirst, camron.hirst@colorado.edu

8 **1. Introduction**

9 The AWAKEN program is a landmark international campaign to collect measurements of
10 wake interactions within wind power plants, spearheaded by the National Renewable Energy
11 Lab (Moriarty et al., 2020). The motivation for this campaign is the poorly understood effect
12 that wake interactions have within wind plants, which leads to significant and unpredictable
13 power and financial losses. High-fidelity, long duration data is being gathered in north-central
14 Oklahoma, an area important and relevant for near-term wind energy developments in the
15 U.S. Great Plains. This data is critical for the development and validation of models which
16 will in turn inform wind development projects and ultimately reduce the cost of wind energy.

17 This project uses doppler lidar data from the AWAKEN project to find and classify low-
18 level jets (LLJs) in the region. LLJs are an important phenomenon to understand and
19 quantify, as they can have a significant effect on wind farm operations. LLJs induce elevated
20 windspeeds across the rotor layer, which increased the overall wind resource. However,
21 increased shear and veer within a LLJ places additional stresses on turbine structures, which
22 can increase operational costs and decrease service life (Kelley, 2011).

23 We analyze data from a doppler lidar located at site H (Figure 1), which is in the
24 immediate vicinity of turbines in the King Plains wind farm. Utilizing the methodology
25 developed in (Vanderwende et al., 2015), three LLJ events are identified between Nov. 9 –
26 Nov. 17 2022. Both northerly and southerly LLJs have been observed, exhibiting
27 characteristics typical for winter months in the area (Whiteman et al., 1997).



28

29 Figure 1: The AWAKEN field experiment layout. In this work, doppler lidar data from
30 site H is used to identify LLJs in the region. Figure adapted from (Debnath et al., 2022)

31 2. Related Works

32 While wind farm technology has seen rapid growth and improvement, there still exist
33 problems to overcome over several scales of space and time. Improved understanding of the
34 physics of atmospheric flow and interaction with wind turbines has been identified as a grand
35 challenge in wind energy research (Veers et al., 2019). Improved understanding of
36 atmospheric flows will inform techniques to maximize the efficiency and therefore cost
37 effectiveness of wind plants.

38 LLJs are an impactful weather event found around the world, driving the transportation of
39 moisture, pollutants, dust, and other airborne substances for thousands of kilometers, all
40 within the atmospheric boundary layer (Rife et al., 2010). Nocturnal migratory birds have
41 been shown to take advantage of LLJs, with southerly winds providing substantial tail winds
42 during the spring migration (Wainwright et al., 2016). These phenomena also impact wind
43 farms, as modern turbines reach heights where LLJs commonly occur. LLJs can increase
44 power output but can also cause damage to wind turbines. The Great Plains region of the
45 United States experiences strong nocturnal LLJs during the warm season, which can be
46 hundreds of kilometers wide and thousands of kilometers long. As this region is also home to
47 much of our wind power resources, understanding LLJs is of great importance.

48

49 One of the first studies of LLJs in the U.S. Great Plains was conducted and presented in
50 (Bonner, 1968). The author used two years of radiosonde data from 46 weather stations to
51 identify hundreds of cases of nocturnal LLJs using a criterion developed therein. The diurnal
52 variation and oscillation of the LLJ was observed throughout the year, although most often in
53 spring and late summer. This landmark study provided substantial proof of the prominence
54 and massive scales of LLJs in the region which significantly impact the local climate.

55 A more recent climatology of LLJs in the Great Plains of the United States provided more
56 detail on general trends in the region (Walters et al., 2008). This study combined forty years
57 of twice-daily radiosonde observations from 36 weather stations across the Great Plains. The
58 authors were able to identify several characteristics of LLJs which vary based on seasonality
59 and location. While this paper helped provide a broad description of LLJs in the region, the
60 authors conclude that much remains to be documented and understood.

61 Other works have studied LLJs in the U.S. Great Plains using lidar measurements. In
62 2013, researchers deployed profiling and scanning lidars to collect data which was used to
63 detect LLJs in central Iowa as part of the CWEX-13 field campaign (Vanderwende et al.,
64 2015). The authors detailed a systematic procedure for computing wind profiles from the
65 scanning lidar and using these profiles to detect and classify LLJs. LLJs were consistently
66 identified, with peak windspeeds around 250-500m at the observation site, heights relevant to
67 modern wind turbines. The authors also investigated the ability of various numerical weather
68 models (and ensembles of said models) to predict LLJs in the area, demonstrating good
69 performance. The LLJ classification procedure will be used in the proposed project to detect
70 LLJs during the AWAKEN experiment.

71 Prior work has studied LLJ climatology in the north-central Oklahoma region (Whiteman
72 et al., 1997), just tens of miles from where the data used in this project was collected. Both
73 southerly and northerly LLJs were observed in the region, the former being much more
74 frequent during the warm season (April – September). Southerly LLJs tend to be lower (300-
75 600m AGL), occur more often at night and exhibit a diurnal clockwise rotation in wind
76 direction and oscillations in speed. Northerly jets were found to be associated with south-
77 bound cold air fronts. They are less dependent on time of day, do not exhibit rotations, and
78 have nose heights that are correlated to distance behind cold fronts. Many of these
79 characteristics were observed in this project.

81 2. Methods

To identify LLJs, this work implements a slightly modified version of the procedure developed in prior work (Vanderwende et al., 2015). The identification of LLJs from lidar measurements is done in three steps:

- 85 1. Initial quality assurance of wind speed and direction measurements at each bin.
 - 86 2. Calculation of wind speed and direction profiles from Lidar radial velocity
 - 87 measurements.
 - 88 3. Identification and classification of LLJs using wind speed profiles.

Wind speed and direction profiles at each altitude were found using a commonly used technique known as velocity azimuth display (VAD). VAD assumes a homogenous flow over the course of a 360-degree azimuth scan. As the Lidar is sweeping the azimuth angles, the radial velocity measurement axis will move in and out of alignment with the horizontal wind vector, resulting in a sinusoidal velocity profile. Using nonlinear least squares, the following function was fit to data at each available altitude bin:

$$v_r = a + b \cos (\theta - \theta_m)$$

96 Where v_r is the radial wind speed, θ is the azimuth angle of the measurement, and
 97 a, b, θ_m are all parameters to be fit. The fitted parameters are then used to derive the
 98 horizontal wind speed and direction using:

$$WS = (u^2 + v^2)^{0.5} = b/\cos\phi$$

$$WD = \theta_m$$

101 Where ϕ is the beam elevation angle from horizontal. To filter out wind speed and
 102 direction datapoint which are poorly fit to the sinusoidal model, we calculate the commonly
 103 used R^2 value as:

$$R^2 = 1 - \frac{SS_{res}}{SS_{tot}}$$

Where SS_{res} is the sum of squares of the residuals, while SS_{tot} is the total sum of squares. A threshold of 0.7 was placed on this metric, as described in (Vanderwende et al., 2015). If a lower value was found, then the wind speed and direction measurement for that altitude was rejected. See Figures 10-12 in the Appendix for examples of valid/invalid VAD fits and their corresponding R^2 values.

110 This procedure can be run for each radial range bin from the Lidar profile. As we know
111 the range r and elevation angle ϕ of the lidar beam (in this work, 60 [deg]), we can derive the
112 AGL altitude h via:

113
$$h = r \cos \phi$$

114 The final step is to classify LLJs based on criteria originally proposed in (Bonner, 1968),
115 then modified by (Whiteman et al., 1997) and (Song et al., 2005). There are two criteria that a
116 wind profile must fulfill to be classified as a LLJ. First, the profile must contain a maximum
117 windspeed above a windspeed threshold, and this maximum windspeed must occur below a
118 height threshold. While Song/Vanderwende impose a 2km threshold, we observed
119 consistently valid data only below 1km in the data available. We therefore placed a height
120 threshold at 1km, and only considered profiles below that threshold. Maximum LLJ nose
121 height observed occurred at 688m, justifying this choice.

122 The second criteria involves a threshold on the reduction of wind speed above the LLJ
123 nose. This shear value must meet a certain threshold for LLJ classification. In (Whiteman et
124 al., 1997), four jet intensity levels (0-3) are specified as a function of maximum windspeed
125 and shear, with thresholds provided in the following table:

126

LLJ Category	Max windspeed [m/s]	Upper shear [m/s]
LLJ-0	≥ 10	≥ 5
LLJ-1	≥ 12	≥ 6
LLJ-2	≥ 16	≥ 8
LLJ-3	≥ 20	≥ 10

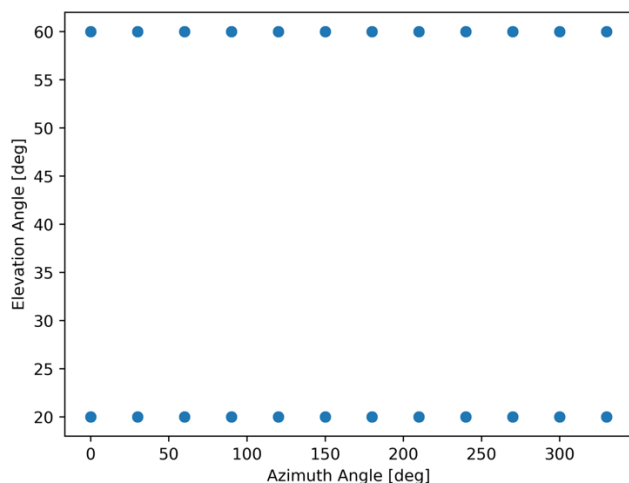
127

128 **3. Results and Discussion**

129

130 Data used in this project was acquired through the DOE's Atmosphere to Electron
131 website (Shi et al.), and can be found at

132 https://a2e.energy.gov/ds/awaken/arm.lidar.sgp_s6.ppi.b1. Unfortunately, only a limited
133 amount of data was able to be acquired from the A2E site via the link above. Therefore, this
134 project examines a dataset composed of measurements taken between Nov 9, 2022, and Nov
135 17, 2022. Lidar measurements are available at approximately 30-minute intervals throughout
136 this period. Measurement azimuth angles ranged from 0 – 360 degrees, at 30-degree intervals.
137 Measurement elevation angles were 20 and 60 degrees (Figure 2). In this work, only
138 measurements at 60-degree elevation were used, however the code could be easily modified
139 to incorporate measurements at 20 degrees elevation.

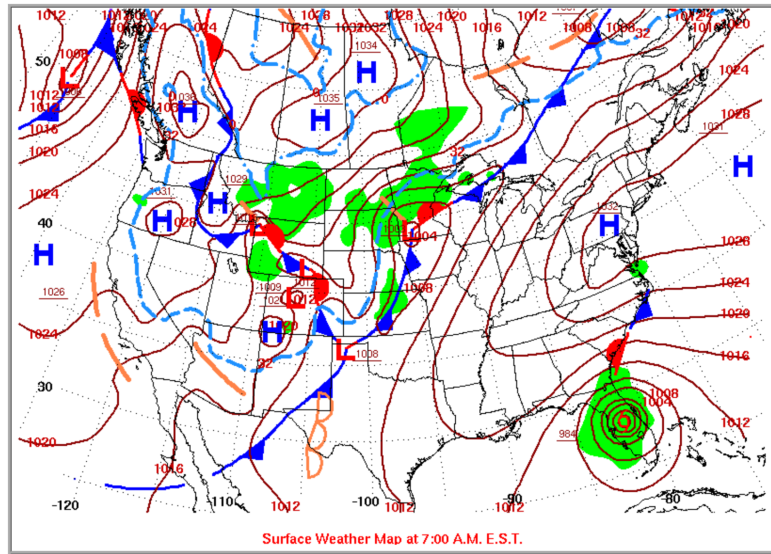


140
141 Figure 2: Elevation and azimuth angles at which measurements are taken by the
142 AWAKEN Site H Doppler Lidar.
143
144 In all, three LLJ events were classified within the data between Nov. 9 – Nov. 17 2022. These
145 events occurred on the 10th, 13th, and 14th and are discussed below.

146 Nov. 10 2022 Event:
147 Around 4 pm CST on Nov. 10 2022, a LLJ was detected by the doppler radar. Initially a
148 class 1, the LLJ continued to develop until reading class 3 around 11pm CST. The
149 development of this LLJ corresponded to a strong south-bound cold front moving through the
150 area (Figure 3). Peak windspeeds reached over 23 m/s. As the LLJ developed, it rose from an
151 initial height of 454m to 668m (Figure 4), which aligns with prior observations of LLJ height
152 growing as a function of distance behind cold front (Whiteman et al., 1997). Winds were
153 approximately southerly during the entire event, exhibiting little turning. See Figure 13 in the
154 Appendix for an example windspeed profile during this event. Little wind direction rotation

155 of the LLJ nose was observed (Figure 5) , which is also consistent with previous northern
156 LLJ observations in the area. Complete time series data for this event can be found in Table 2
157 in the Appendix.

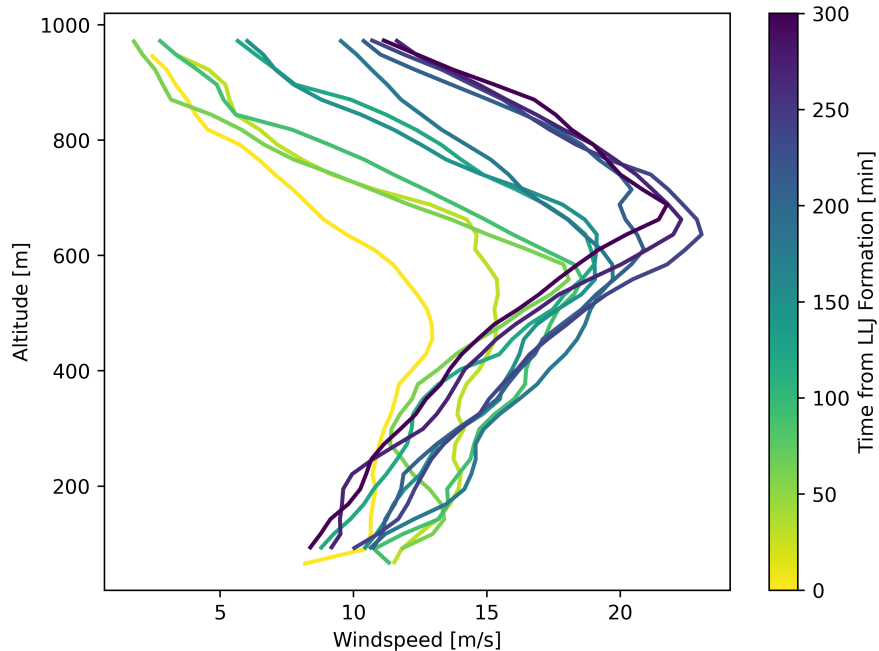
158



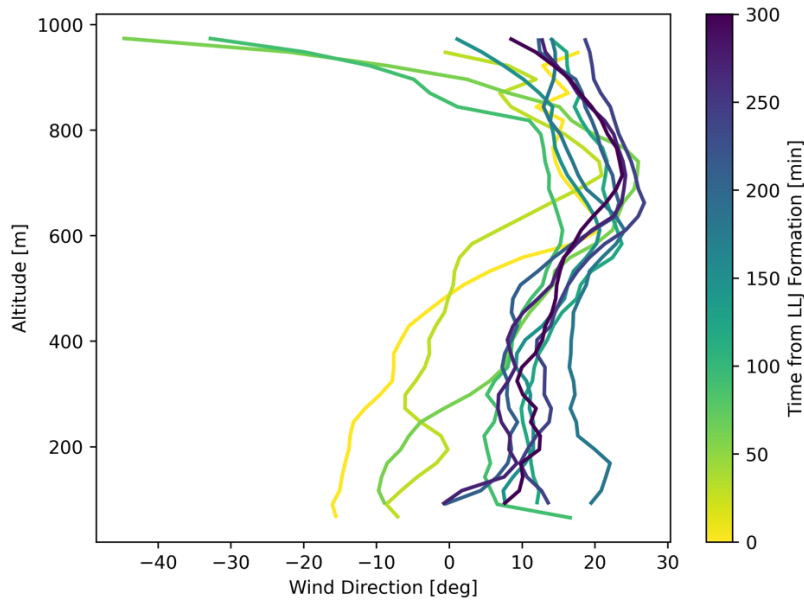
159 Figure 3: Screenshot of weather map on Nov. 10, 2022. A south-bound cold front can be
160 seen moving across north-central Oklahoma, corresponding to the formation of a northerly
161 LLJ. Adapted from: http://www.wpc.ncep.noaa.gov/dailywxmap/index_20221110.html

162

163 Figure 4: Evolution of windspeed during the Nov. 10 2022 LLJ event. Increasing nose
164 height was observed as the south-bound cold front moved away from the observation site.



165



166

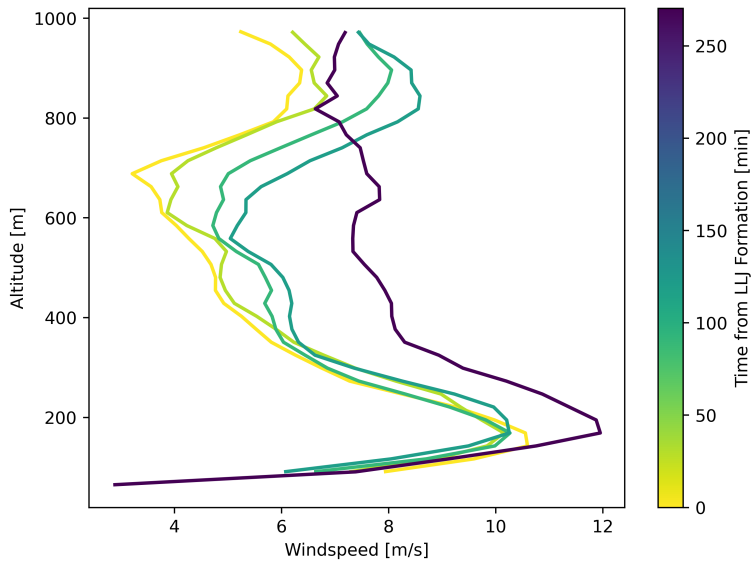
167 Figure 5: Evolution of wind direction during the Nov. 10 2022 LLJ event. Relatively little
168 change in LLJ nose wind direction was observed. Strong wind veer was found aloft (near
169 1000m)

170

171 Nov. 13, 2022 Event:

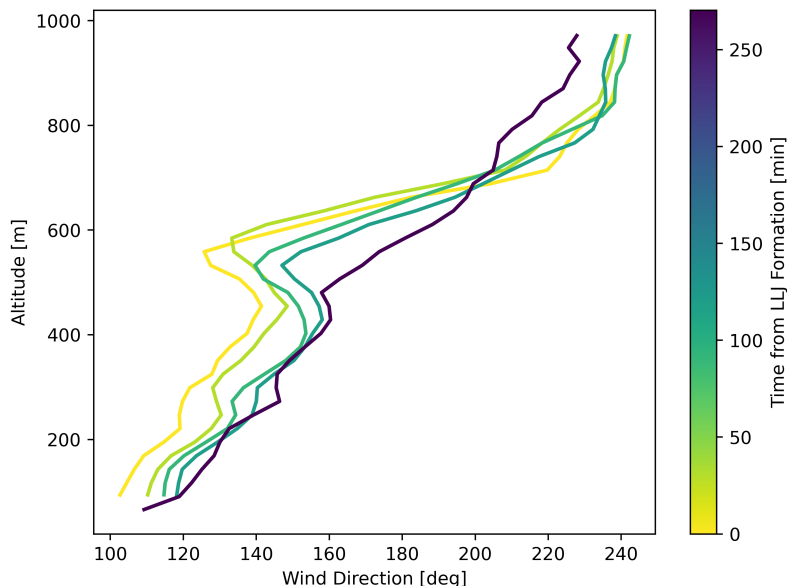
172 A weaker LLJ was detected on Nov. 13, 2022. This LLJ originated around 1:30 am CST
173 and persisted sporadically until 6 am CST. Maximum windspeeds reached just under 12 m/s,
174 with winds originating from the southeast. The reason for sporadic classification was profiles
175 were on the cusp of being classified as LLJ-0 (Table 2; Figures 14 and 15 in Appendix).
176 Oscillatory windspeeds in southerly LLJs have been observed in prior observations, but have
177 longer periods as part of the diurnal cycle (Whiteman et al., 1997). This event also occurred
178 at a very low altitude of just 168m AGL maximum (Figure 6), which indicates potential
179 impact on wind turbines. The data also indicated significant wind shear below 200m AGL,
180 which could cause increased wear on local wind turbines. Little wind direction rotation was
181 observed over the event, although significant wind veer was found from ground level to
182 1000m AGL (Figure 7). Complete time series data for this event can be found in Table 3 in
183 the Appendix.

184



185

186 Figure 6: Evolution of windspeed during the Nov. 13 2022 LLJ event. Oscillation around
187 the 10 m/s threshold was observed over ~5 hours.



188

189 Figure 7: Evolution of wind direction during the Nov. 13 2022 LLJ event. Nose height is
190 observed to increase as the south-bound cold front moves away.

191

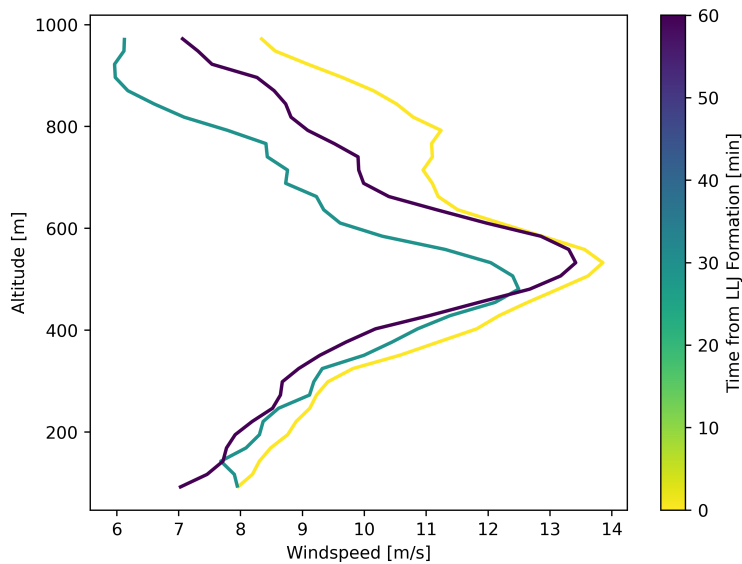
192

193 Nov. 14 2022 Event:

194 The final LLJ event was detected on Nov. 13, 2022. This LLJ originated around 7:00 am
195 CST, and persisted just an hour until 8:00 am CST. Maximum windspeeds reached just under
196 14 m/s, with nose height around 500m AGL and winds originating from the south. Once

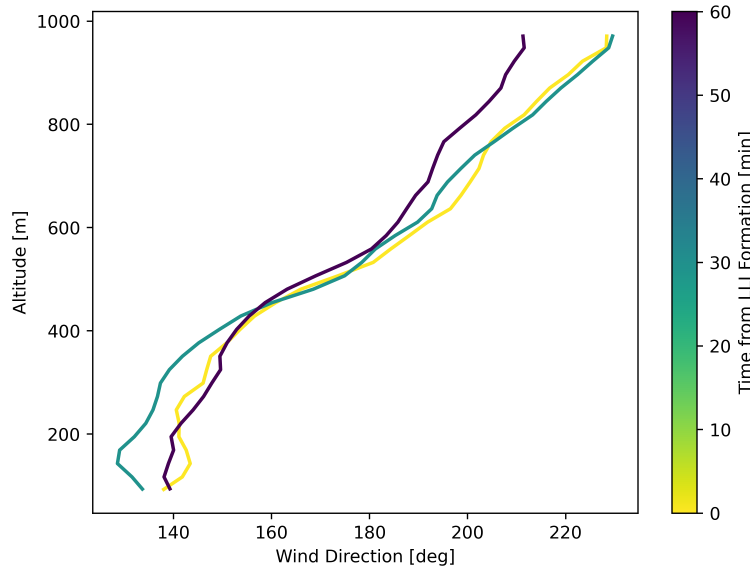
197 again, fast oscillations in windspeeds were observed (Figure 8). Little change in nose wind
198 direction was observed (Figure 9), likely due to the short time span of the event. Significant
199 wind veer was observed from 400m to 1000m AGL. Complete time series data for this event
200 can be found in Table 4 in the Appendix.

201



202

203 Figure 8: Evolution of windspeed during the Nov. 14 2022 LLJ event. Oscillation around
204 the 10 m/s threshold was observed over ~5 hours.



205

206 Figure 9: Evolution of wind direction during the Nov. 13 2022 LLJ event. Nose height is
207 observed to increase as the south-bound cold front moves away.
208

209 4. Conclusion and Future Work

This work used doppler lidar data to detect and classify low-level jets using the methods presented in (Vanderwende et al., 2015) and prior works. In total, 3 LLJ events were identified at site H of the AWAKEN experiment between Nov. 9 – 17, 2022. The LLJs observed exhibited characteristics that were largely consistent with prior observations (Whiteman et al., 1997). The LLJs were found within and around wind farms, thus may have distinct impacts on wind farm performance.

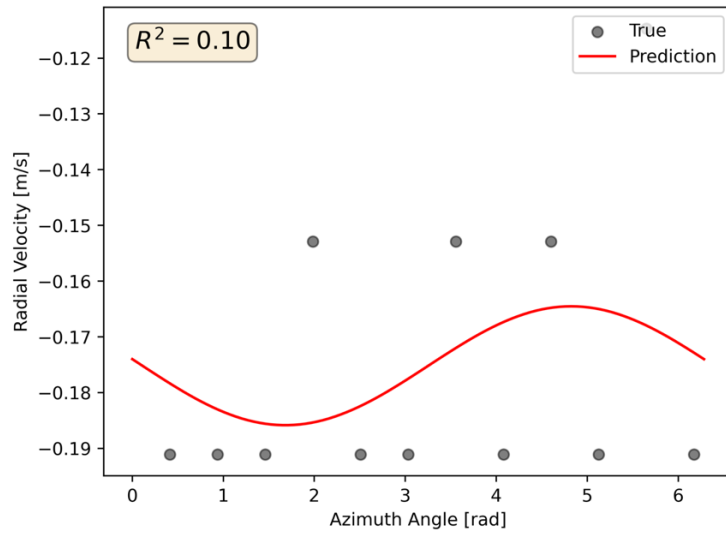
This project was limited in scope. There are several notable extensions that could readily be investigated. First, a study investigating the dependence of LLJ formation and severity as a function of atmospheric stability should be done. This project did not have temperature profile data available, making atmospheric stability calculations difficult. Second, it may be interesting to see how well an NWP model could predict the observed LLJs in the area. This could validate whether NWP models can be used for predictive control of wind farms. Third, an investigation into LLJ occurrence over a longer period would be interesting and informative. Is LLJ climatology changing over time? The code developed in this project could be readily used to analyze a larger dataset, when it becomes available. Finally, the lidar measurements in this study were taken near the King Plains wind farm (Figure 1). An investigation into the effect of the wind farm on local LLJ formation should be conducted, as the wind farm likely influences our ability to detect local low-altitude LLJs when taking measurements down wind.

ACKNOWLEDGEMENTS

230 The author acknowledges the code contributions from Daphne Quint and Prof. Julie
231 Lundquist, which helped kick-start the project. All code to recreate the results can be found
232 on GitHub at: https://github.com/CameronAlexanderHirst/ATOC5770_LLJ.

APPENDIX

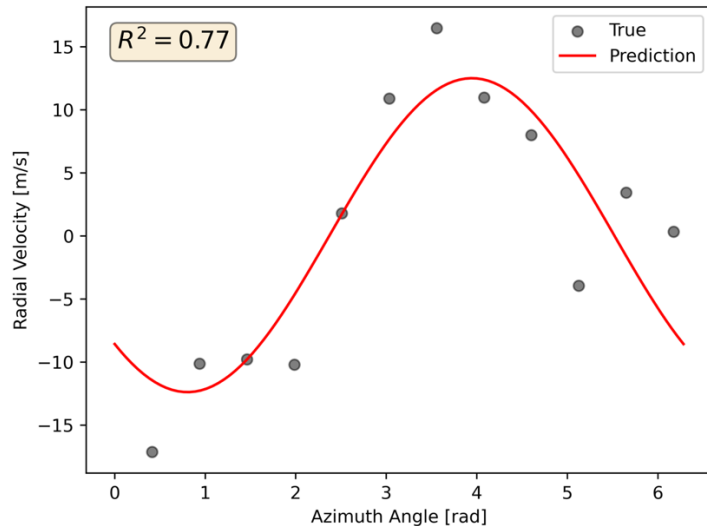
LLJ Figures



236

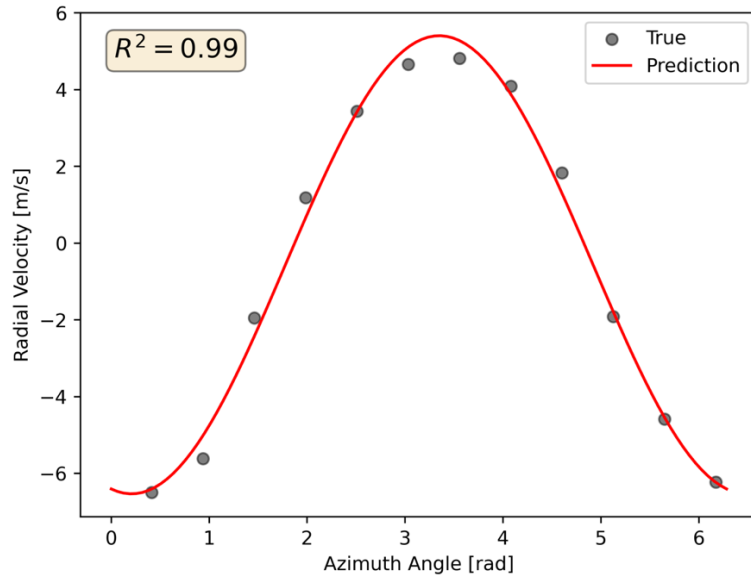
237 Figure 10: VAD Fit of Lidar scan on Nov. 11 2022 at 12m AGL. R-squared value does
238 not meet the 0.7 threshold, therefore the windspeed and wind direction measurement was
239 rejected.

240



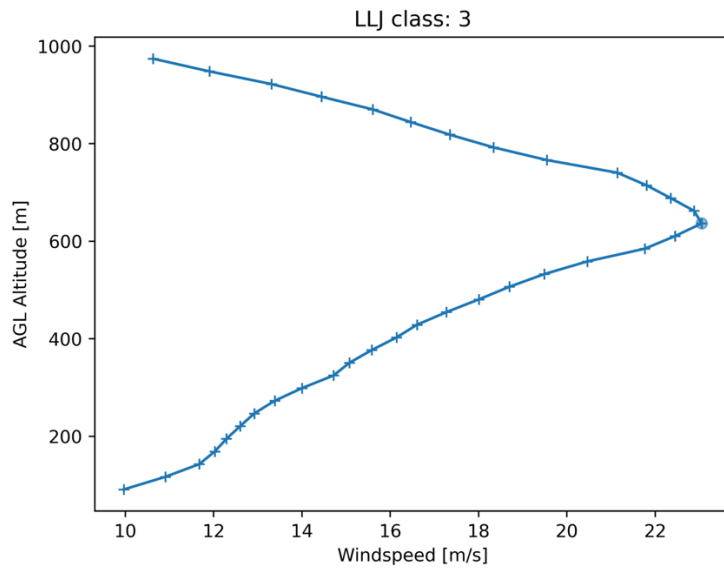
241

242 Figure 11: VAD Fit of Lidar scan on Nov. 11 2022 at 2325m AGL. R-squared value
243 meets the 0.7 threshold, therefore the windspeed and wind direction measurement was
244 accepted.



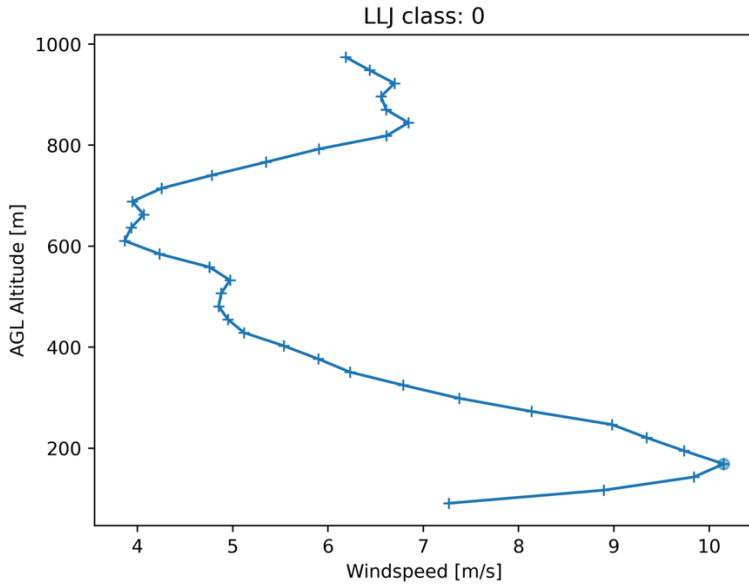
245

246 Figure 12: VAD Fit of Lidar scan on Nov. 11 2022 at 142m AGL. R-squared value meets
247 the 0.7 threshold, therefore the windspeed and wind direction measurement was accepted.



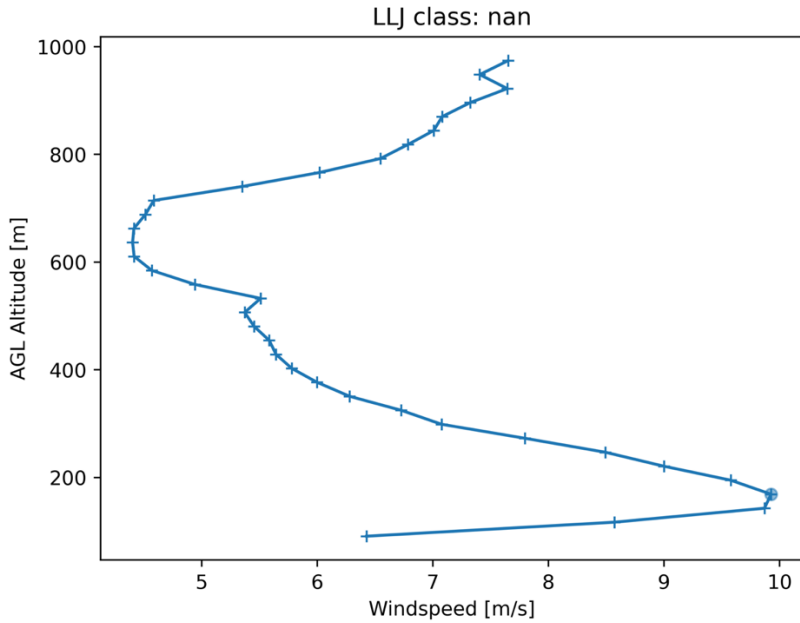
248

249 Figure 13: A windspeed profile taken on Nov 10 2022. This profile is a distinct example
250 of LLJ formation, with maximum windspeed exceeding 22 m/s. This profile was classified as
251 LLJ-3.



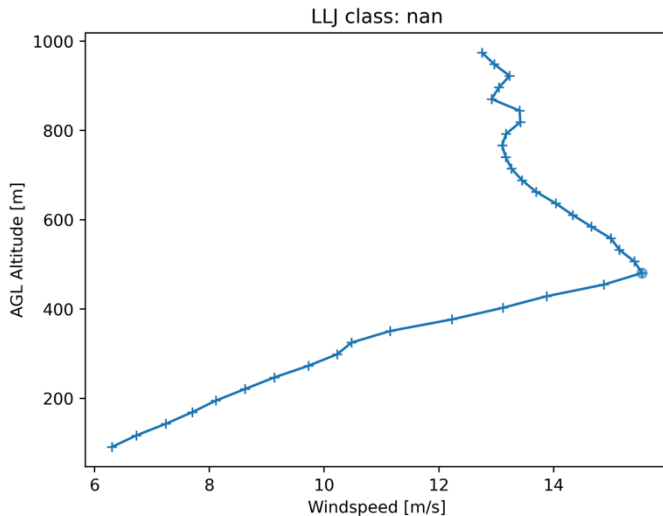
252

253 Figure 14: A windspeed profile taken at 8:00am UTC on Nov 13, 2022. This profile met
 254 the windspeed threshold of 10 m/s to be classified as LLJ-0. Similar profiles resulted during
 255 the Nov 13 event, leading to sporadic LLJ identification.



256

257 Figure 15: A windspeed profile taken at 8:30am UTC on Nov 13, 2022. This profile did
 258 not meet the windspeed threshold of 10 m/s to be classified as an LLJ. Similar profiles
 259 resulted during the Nov 13 event, leading to sporadic LLJ identification.



260

261 Figure 16: A windspeed profile taken on Nov. 14 2022. This profile did not meet the
262 shear criteria to be classified as an LLJ.

263

264

Table 2: Nov. 10 2022 Low-Level Jet Event

Time [UTC]	LLJ Class	Nose Height [m]	Upper Shear [m/s]	Max. WS [m/s]	Wind Direction [deg]
2022-11-10 22:00:21	1	454.66	10.55	12.95	-3.24
2022-11-10 22:30:03	1	532.61	12.08	15.42	0.71
2022-11-10 23:00:21	2	558.59	16.35	18.07	16.57
2022-11-10 23:30:03	2	558.59	15.89	18.58	14.13
2022-11-11 00:00:21	2	584.57	13.43	19.03	23.69
2022-11-11 00:30:04	2	636.53	13.16	19.12	19.98
2022-11-11 01:00:21	2	558.59	10.26	19.73	20.96
2022-11-11 01:30:04	3	610.55	10.57	20.89	19.80

2022-11-11 02:00:21	3	636.53	12.42	23.05	25.92
2022-11-11 02:30:03	3	662.51	10.72	22.29	23.65
2022-11-11 03:00:21	3	688.49	10.69	21.76	22.91

265

266

Table 3: Nov. 13 2022 Low-Level Jet Event

Time [UTC]	LLJ Class	Nose Height [m]	Upper Shear [m/s]	Max. WS [m/s]	Wind Direction [deg]
2022-11-13 07:30:03	0	142.89	7.38	10.59	106.56
2022-11-13 08:00:21	0	168.87	6.29	10.15	116.64
2022-11-13 08:30:03			5.52	9.93	
2022-11-13 09:00:21	0	168.87	5.55	10.27	120.19
2022-11-13 09:30:03	0	168.87	5.21	10.25	123.61
2022-11-13 10:00:20			4.63	9.84	
2022-11-13 10:30:04			4.38	10.28	
2022-11-13 11:00:21			4.93	11.02	
2022-11-13 11:30:03			4.71	11.43	
2022-11-13 12:00:21	0	168.87	5.32	11.95	128.43

267

268

Table 4: Nov. 13 2022 Low-Level Jet Event

Time [UTC]	LJ Class	Nose Height [m]	Upper Shear [m/s]	Max. WS [m/s]	Wind Direction
2022-11-14 13:00:21	0	532.61	5.54	13.85	180.74
2022-11-14 13:30:03	1	480.64	6.53	12.49	168.52
2022-11-14 14:00:21	1	532.61	6.38	13.42	175.31

269

270

REFERENCES

- 271 Bonner, W. D. (1968). CLIMATOLOGY OF THE LOW LEVEL JET. *Monthly Weather*
 272 *Review*, 96(12), 833–850. [https://doi.org/10.1175/1520-0493\(1968\)096<0833:COTLLJ>2.0.CO;2](https://doi.org/10.1175/1520-0493(1968)096<0833:COTLLJ>2.0.CO;2)
- 273 Debnath, M., Scholbrock, A. K., Zalkind, D., Moriarty, P., Simley, E., Hamilton, N., Ivanov,
 274 C., Arthur, R. S., Barthelmie, R., Bodini, N., Brewer, A., Goldberger, L., Herges, T.,
 275 Hirth, B., Valerio Iungo, G., Jager, D., Kaul, C., Klein, P., Krishnamurthy, R., ...
 276 Wharton, S. (2022). Design of the American Wake Experiment (AWAKEN) field
 277 campaign. *Journal of Physics: Conference Series*, 2265(2), 022058.
 278 <https://doi.org/10.1088/1742-6596/2265/2/022058>
- 279 Kelley, N. D. (2011). *Turbulence-Turbine Interaction: The Basis for the Development of the*
 280 *TurbSim Stochastic Simulator* (NREL/TP-5000-52353, 1031981; p. NREL/TP-5000-
 281 52353, 1031981). <https://doi.org/10.2172/1031981>
- 282 Moriarty, P., Hamilton, N., Debnath, M., Herges, T., Isom, B., Lundquist, J., Maniaci, D.,
 283 Naughton, B., Pauly, R., Roadman, J., Shaw, W., van Dam, J., & Wharton, S. (2020).
 284 *American WAKE experimeNt (AWAKEN)* (NREL/TP-5000-75789, 1659798,
 285 MainId:5894; p. NREL/TP-5000-75789, 1659798, MainId:5894).
 286 <https://doi.org/10.2172/1659798>

- 288 Rife, D. L., Pinto, J. O., Monaghan, A. J., Davis, C. A., & Hannan, J. R. (2010). Global
289 Distribution and Characteristics of Diurnally Varying Low-Level Jets. *Journal of*
290 *Climate*, 23(19), 5041–5064. <https://doi.org/10.1175/2010JCLI3514.1>
- 291 Song, J., Liao, K., Coulter, R. L., & Lesht, B. M. (2005). Climatology of the Low-Level Jet at
292 the Southern Great Plains Atmospheric Boundary Layer Experiments Site. *Journal of*
293 *Applied Meteorology*, 44(10), 1593–1606. <https://doi.org/10.1175/JAM2294.1>
- 294 Vanderwende, B. J., Lundquist, J. K., Rhodes, M. E., Takle, E. S., & Irvin, S. L. (2015).
295 Observing and Simulating the Summertime Low-Level Jet in Central Iowa. *Monthly*
296 *Weather Review*, 143(6), 2319–2336. <https://doi.org/10.1175/MWR-D-14-00325.1>
- 297 Veers, P., Dykes, K., Lantz, E., Barth, S., Bottasso, C. L., Carlson, O., Clifton, A., Green, J.,
298 Green, P., Holttinen, H., Laird, D., Lehtomäki, V., Lundquist, J. K., Manwell, J.,
299 Marquis, M., Meneveau, C., Moriarty, P., Munduate, X., Muskulus, M., ... Wiser, R.
300 (2019). Grand challenges in the science of wind energy. *Science*, 366(6464),
301 eaau2027. <https://doi.org/10.1126/science.aau2027>
- 302 Wainwright, C. E., Stepanian, P. M., & Horton, K. G. (2016). The role of the US Great Plains
303 low-level jet in nocturnal migrant behavior. *International Journal of Biometeorology*,
304 60(10), 1531–1542. <https://doi.org/10.1007/s00484-016-1144-9>
- 305 Walters, C. K., Winkler, J. A., Shadbolt, R. P., van Ravensway, J., & Bierly, G. D. (2008). A
306 Long-Term Climatology of Southerly and Northerly Low-Level Jets for the Central
307 United States. *Annals of the Association of American Geographers*, 98(3), 521–552.
308 <https://doi.org/10.1080/00045600802046387>
- 309 Whiteman, C. D., Bian, X., & Zhong, S. (1997). Low-Level Jet Climatology from Enhanced
310 Rawinsonde Observations at a Site in the Southern Great Plains. *Journal of Applied*

311 *Meteorology*, 36(10), 1363–1376. [https://doi.org/10.1175/1520-0450\(1997\)036<1363:LLJCFE>2.0.CO;2](https://doi.org/10.1175/1520-0450(1997)036<1363:LLJCFE>2.0.CO;2)

313